Available online at www.sciencedirect.com
ScienceDirect
Carbohydrate Polymers 73 (2008) 55–63
Carbohydrate Polymers
www.elsevier.com/locate/carbpol

# Physical and mechanical properties of thermoplastic starch/montmorillonite nanocomposite films

Viviana P. Cyras [a], Liliana B. Manfredi [a], Minh-Tan Ton-That [b], Analía Vázquez [a,*]

[a] *Institute of Material Science and Technology (INTEMA), University of Mar del Plata – National Research Council (CONICET), Av. Juan B. Justo 4302 – B7608FDQ – Mar del Plata, Argentina*

[b] *Industrial Material Institute, National Research Council Canada, 75 Mortagne Blvd, Boucherville, Que., Canada J4B 6Y4*

Received 9 December 2006; received in revised form 20 July 2007; accepted 5 November 2007
Available online 21 November 2007

**Abstract**

Glycerol-plasticized starch/clay nanocomposites films were prepared from potato starch and three different loadings of montmorillonite aqueous suspensions by casting, to study the effect of the nanoclay in the properties of starch. The clay dispersion in the films was analyzed by X-ray diffraction (XRD). It was observed that the 001 diffraction peak of clay was shift to lower angles in the nanocomposites patterns providing strong evidence that the clay nanolayers formed an intercalated structure but not complete exfoliation. An improvement in the thermal resistance of starch with the addition of clay was also observed by means of thermogravimetric analysis (TGA). The water absorbed by the nanocomposites measured in an environment with a 75% of constant relative humidity was reduced by the addition of montmorillonite to the starch. The micro-tensile test was performed on the nanocomposite films showing significant improvement in the Young modulus up to 500% for the nanocomposite containing 5 wt% of clay.


*Keywords:* Thermoplastic starch; Clay; Nanocomposites

## 1. Introduction

In order to solve problems generated by plastic waste many efforts have been done to obtain an environmental friendly material. Most of the research investigation is focused on substitute petro-based plastics by biodegradable materials with similar properties in a low cost and effective manner. Starch is a biodegradable polymer produced in abundance from many renewable resources. As a consequence it is easily available and very cheap. Starch is the major form of stored carbohydrate in plants, being the end product of photosynthesis (Charles, Kao, & Huang, 2003; Plackett & Vázquez, 2004; Singh, Pandey, Rutot, Degée, & Dubois, 2003).

Starch is a semicrystalline polymer and it is composed of two polymers with repeating α-D-glucopyranosyl units. These substances are amylase and amylopectin, a linear and a highly branched polysaccharide, respectively. The repeating units in amylase are linked by α (1–4) linkages. The amylopectin has an α (1–4) linked backbone and about 5% α (1–6) linked branches (Cheetham & Tao, 1998; Svensson & Eliasson, 1995). In native form, starch granules are insoluble in cold water and most uses involve a heating treatment in the presence of excess of water. Below a critical temperature (about 60 °C), that is the so-called gelatinization temperature, starch granules absorb water and undergo swelling to many times their original size. This process is attributed to the diffusion of amylose outside the granule. Beyond this critical temperature, the swollen starch granules can undergo a disruption into smaller aggregates or particles, and result in a gelatinized starch. The thermoplastic starch or plasticized starch is obtained after disruption and plasticization of native starch, by temperature and in presence of water and another plasticizer, such as glycerol. However, the thermoplastic starch has

* Corresponding author. Tel.: +542234816600; fax: +542234810046.
*E-mail address:* anvazque@fi.mdp.edu.ar (A. Vázquez).

0144-8617/$ - see front matter © 2007 Elsevier Ltd. All rights reserved.
doi:10.1016/j.carbpol.2007.11.014

some limitations: it is mostly water-soluble and has poor resistance and low strength. The resistance to water may be improved by adding certain synthetic polymers (Bastioli, 1995), inorganic materials (Huang, Yu, Ma, & Peng, 2005; Ray & Okamoto, 2003) or lignin (Baumberg, Lapierre, Monties, & Della Valle, 1998). In addition, it is possible to improve the mechanical properties to this polymer by the addition of fillers. These composites could be use in packaging where good barrier and thermal properties are required (Plackett & Vázquez, 2004; Singh et al., 2003; Svensson & Eliasson, 1995).

Development of the polymer/clay nanocomposites is one of the latest revolutionary steps of the polymer technology. Preparations of blends or nanocomposites using inorganic or natural fibers are among the routes to improve some of the properties of biodegradable polymers. The nanocomposites obtained by the addition of low percentages of clay to polymers exhibited an improvement in the properties such as barrier, thermal and oxidative when compared with traditional composites. Clay minerals are aluminum silicates of a layered type classified as phyllosilicates. Montmorillonite is among the most commonly used layered silicates because it is environmentally friendly and readily available in large quantities with relatively low cost. Montmorillonite crystal lattice consists of 1 nm thin layers with an octahedral alumina sheet sandwiched between two tetrahedral silica sheets. The aspect ratio is about 100. The stacking of the platelets leads to a Van der Waals gap or gallery between the layers. The layers are negatively charged and this charge is balanced by alkali cations such as $Na^+$, $Li^+$ or $Ca^{2+}$ in the gallery between the aluminosilicate layers. The Na-montmorillonite clay is hydrophilic with a high surface area (Ray & Okamoto, 2003; Tjong, 2006). The improvement in the polymer properties was reached when the clay is exfoliated and the major problem in preparing these composites is to separate the layers of the clay because they are initially agglomerated. Therefore, it is possible to improve the properties of starch by the addition of small amounts of environmentally friendly filler, to use the starch in more special or severe situations (Huang et al., 2005; Pukánszky, Müller, & Bagdi, 2006; Ray & Okamoto, 2003).

The aim of this work is to study the influence of the addition of low percentages of clay on the barrier, thermal and mechanical properties of plasticized starch.

## 2. Experimental

### 2.1. Materials

Native potato starch was kindly provided by AVEBE, Argentina S.A. (Buenos Aires, Argentina). Glycerol was purchased from Aldrich, USA. Sodium montmorillonite (Cloisite® $Na^+$) with a cation exchange capacity (CEC) of 92.6 meq/100 g clay was supplied by Southern Clay Products (Texas, USA).

### 2.2. Preparation of plasticized starch/montmorillonite nanocomposites films

On one hand, native starch was dispersed in distilled water with 30 wt% of glycerol. Then the suspension was heated to 70 °C for 15 min under continuous stirring to gelatinize the potato starch granules. On the other hand, the montmorillonite (MMT) was dispersed in distilled water by sonication during 10 min at room temperature. The clay dispersion was added to the aqueous dispersion of starch and the mixture was continued to sonicate for another 30 min at room temperature. Then, the films were obtained by casting pouring the hot suspension into rectangular moulds and vaporating it in an oven at 45 °C until constant weight was reached. The starch/clay ratios were 100/0, 98/2, 97/3 and 95/5 wt/wt, relative to dry starch. The films were stored at room temperature in a vacuum desiccator for 6 weeks in order to obtain reproducible results. The thickness of the films was $0.25 \pm 0.04$ mm.

### 2.3. Methods

XRD analyses of the composites were performed in a Bruker Discover 8 diffractometer operating at 40 kV and 40 mA with $CuK_\alpha$ radiation ($\alpha = 1.54$ Å). The crystallinity was determined dividing the crystalline area by the total (crystalline + amorphous) area (Cyras, Tolosa Zenklusen, & Vázquez, 2006).

TGA was performed on the specimens with a Shimadzu thermal analyzer at a heating rate of 10 °C/min under nitrogen atmosphere. The specimen weight was in the 7–15 mg range.

The contact angle measurement was made by the sessile drop method. Drops of ethylene glycol (Aldrich, 99.1%) and di-iodomethane (Aldrich, 99%) were formed on the surfaces of the film specimens. The contact angles made by the drops of these liquids were measured with a camera MV-50, zoom 6× and acquired with the software Image NIH. At least five drops per liquid were measured. To determine the total surface energy of the materials and their polar and dispersive components, the Owens and Went equation (Gutowski, 1991) was used:

$$0.5\gamma_2(1+\cos\theta) = (\gamma_1^d\gamma_2^d)^{\frac{1}{2}} + (\gamma_1^p\gamma_2^p)^{\frac{1}{2}} \quad (1)$$

where 1 and 2 refers to the solid and liquid, respectively; $\gamma^d$ is the dispersive component and $\gamma^p$ the polar component of the surface energy; $\theta$ is the contact angle. If the contact angles made by two liquids of known $\gamma^d$ and $\gamma^p$ are measured, it is possible to solve the Eq. (1) and infer the $\gamma_1^d$ and $\gamma_1^p$ for the material. Then, the total surface energy is estimated from Eq. (2):

$$\gamma_1 = \gamma_1^d + \gamma_1^p \quad (2)$$

The surface energy components of probe liquids used for the contact angle measurements are listed in Table 1.

The samples were dried until constant weight in an oven to remove the moisture before water absorption testing by

Table 1
Surface energy components of probe liquids for contact angle measurements (Shimizu & Demarquette, 2000)

| (mN/m) | Ethylene glycol | Diiodomethane |
|---|---|---|
| Total surface energy ($\gamma$) | 47.7 | 50.8 |
| Dispersive component ($\gamma^d$) | 30.1 | 48.5 |
| Polar component ($\gamma^p$) | 17.6 | 2.3 |

gravimetric method. This weight was taken as initial weight ($w_0$). The samples were kept in a 75% constant relative humidity environment generated in a hermetic glass container with aqueous saturated NaCl solutions (ASTM E 104–85). The mass of the samples was weighed at different times ($w_t$).

Infrared Spectroscopy with Fourier Transformed technique (FTIR) was performed on the specimen using a Mattson mod Genesis 2, in DRIFT mode, using 32 scans at 2 $cm^{-1}$ resolution. The 2933 $cm^{-1}$ peak corresponding to the absorption of the $CH_2$ group present in the starch was used as internal standard because it does not change after the addition of clay.

Transmission optical microscopy (TOM) was performed on the starch and nanocomposite films employing a Leica DMLB microscope, with crossed polarizers, provided with a video camera Leica DC 100.

Test specimens were cut from the films obtained by casting, using the punch to obtain a dog-bone sample following ASTM D882-97. The samples were subjected to micro-tensile test on an Instron Universal Testing Machine, Model 1123, at 23 °C and 90% HR. The crosshead speed was 1 mm/min and an extensometer video F.O.V.: 50 mm was used in the measurements.

Scanning electronic microcopy (SEM) was performed on the fracture surfaces of the specimens. The films surface was coated with a 300 Å gold layer and observed in a Hitachi S-4700 microscope.

## 3. Results and discussion

In order to investigate the dispersion of the montmorillonite layers, X-ray diffraction analyses were performed on the composites. Fig. 1 shows the XRD patterns obtained for the starch, the MMT and the nanocomposites. Starch shows no peak in the study range while MMT exhibits a single 001 diffraction peak around 7.3°. In the composite films the 001 diffraction peak of the MMT (12.1 Å) was shifted to lower angles regardless the clay content. These results should indicate that either the glycerol or the polymer chains or both entered into the silicate layers forming intercalated starch/MMT nanocomposites, without reaching complete exfoliation. This could be due to the strong polar interactions between the hydroxyl groups present both in the polymer chain, in the glycerol and in the silicate layers (Park et al., 2002).

Thermal analysis was performed in order to determine if the addition of clay produces any change on the thermal decomposition behavior of starch. TGA of starch, MMT and nanocomposites films up to 400 °C are shown in Fig. 2. The DTG curves show an initial peak in the temperature range from 30 to 200 °C that represents the evaporation of water adsorbed by starch and MMT, the glycerol used, together with the evaporation of low molecular weight compounds. At about 291 °C the starch decomposition was observed. This peak shifted to higher temperatures in the nanocomposites, indicating that the introduction of clay improve the thermal stability of starch by approximately 25 °C. The DTG curve of the MMT only

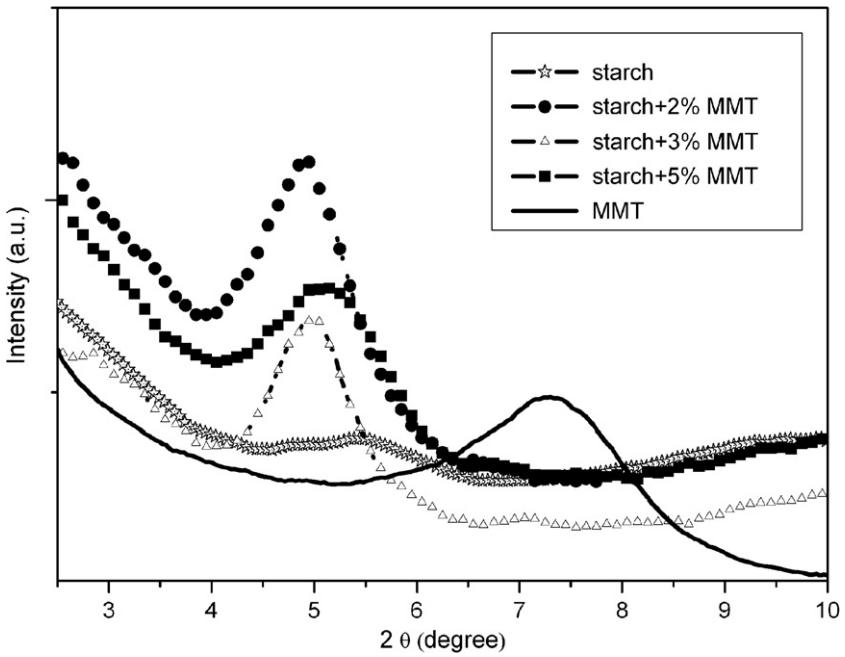


Fig. 1. XRD patterns for the starch, MMT and their composites.

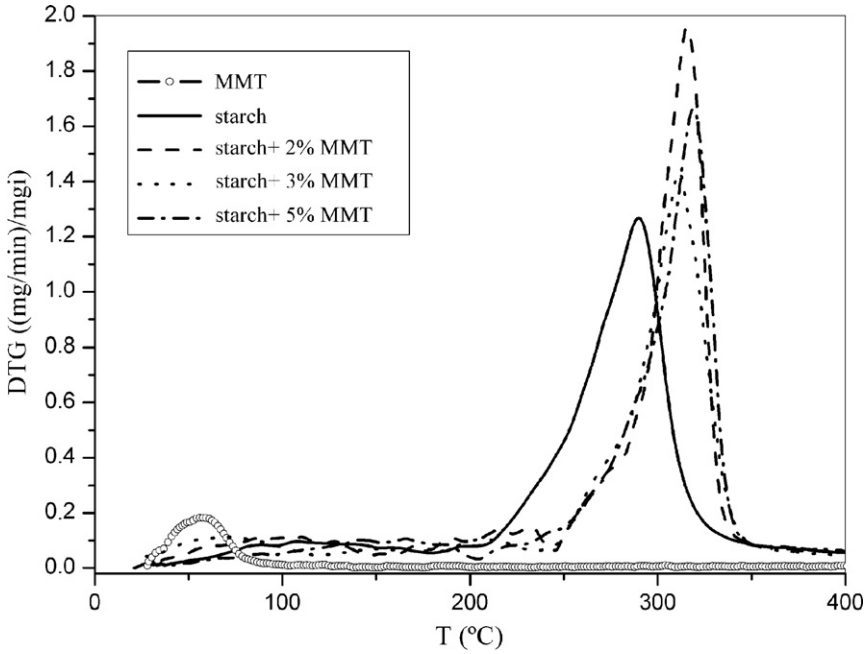


Fig. 2. Thermogravimetric curves of films of starch, MMT and its nanocomposites.

Table 2
Contact angle measured on the films surfaces

| Films | Ethylene glycol | Diiodomethane |
|---|---|---|
| Starch | 49.46 ± 1.60 | 43.71 ± 1.39 |
| Starch + 2% MMT | 36.75 ± 3.35 | 44.36 ± 3.17 |
| Starch + 3% MMT | 40.50 ± 3.55 | 47.19 ± 2.28 |
| Starch + 5% MMT | 32.16 ± 0.70 | 42.63 ± 2.26 |

revealed the loss of water at the very beginning of the degradation process showing its great thermal stability in the temperature range analyzed. The inorganic material has better thermal stability than the organic material due to its chemistry. The clay acts as a heat barrier, which enhances the overall thermal stability of the composites. Consequently, the incorporation of inorganic particles improved the thermal stability of starch.

The contact angle method was used to compare the hydrophilic character of the composites by measuring their surface energy. The contact angle made by the drops of the reference liquids on the films surfaces are shown in Table 2. The polar and dispersive components of the surface energy calculated by means of the Owens and Went equation (Gutowski, 1991) for the starch and their nanocomposites are shown in Fig. 3. A diminution of the dispersive components was observed, as well as an increment in the polar component of the surface energy with the addition of MMT to the system. This behavior could be due to the hydroxylated silicate layers that make the MMT a hydrophilic compound, as well as the surface morphology.

FTIR spectra of starch/glycerol films and their composites in the range of 3200–3800 $cm^{-1}$ are given in Fig. 4. All spectra showed a broad peak in this region that corresponds to the O–H stretching but some differences arisen. In the spectra of the composites could be distinguished two peaks. The one that appeared at approximately 3650 $cm^{-1}$ corresponds to the free hydroxyl groups and the other one at 3530 $cm^{-1}$ is characteristic of the hydroxyl groups that participate in the formation of hydrogen bonds (Lin-Vien, Colthup, Fateley, & Grasselli, 1991). It was observed that the composites are the ones that contained higher quantity of free hydroxyl groups than the starch, because of the higher height of the peak at 3650 $cm^{-1}$ compared to that at 3530 $cm^{-1}$. This result is in accordance with the higher hydrophilic character of the composites compared to the films of starch observed by the contact angle method.

The moisture content as a function of time was determined in order to measure the equilibrium moisture content of starch and nanocomposite films. Fig. 5 shows the moisture content ($w$%) at 25 °C, calculated as follows:

$$w\% = \frac{w_t - w_0}{w_0} \times 100 \quad (3)$$

where, $w_t$ is the wet weight of films at each time and $w_0$ is the initial weight of dry film.

It was observed that the equilibrium water content of nanocomoposites was less than that of starch film, at an environmental relative humidity of 75%. These results indicated that the addition of clay improve the water resistance of starch. The reason could be that the starch is able to form hydrogen bonds with the hydroxyls of the MMT layers and this strong structure could reduce the diffusion of water molecules in the material. Similar results were obtained by other authors who observed a diminution in the water absorbed by nanocomposites made with MMT or kaolin compared with the native starch (Carvalho,

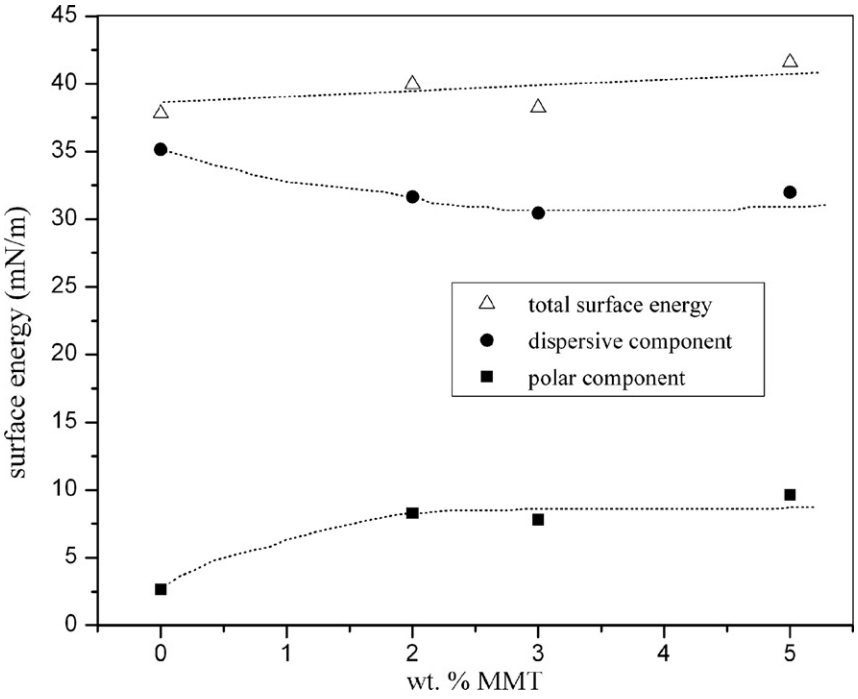


Fig. 3. Surface tension and its components in function of MMT content in the films.

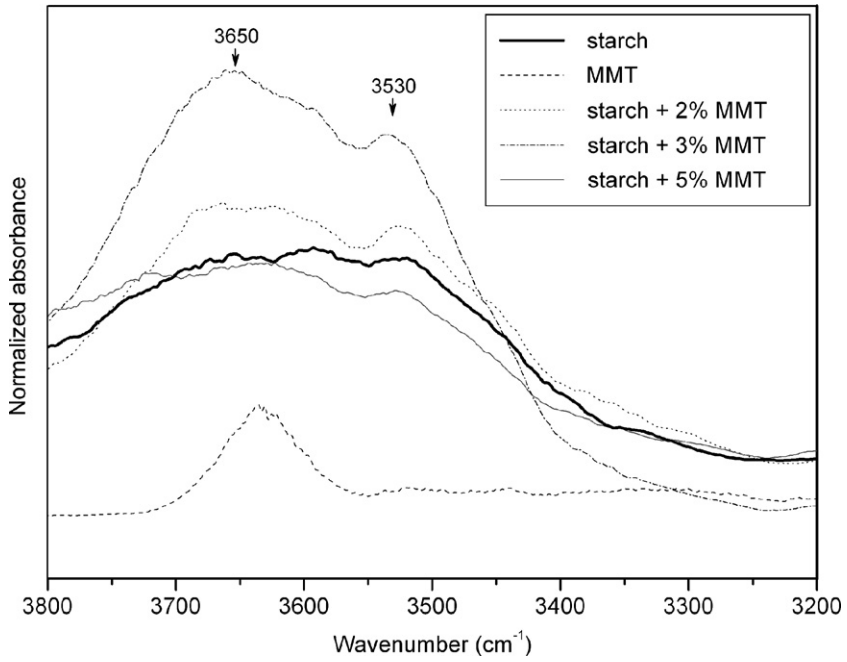


Fig. 4. FTIR spectra of the starch and its composites in the range 3200–3800 $cm^{-1}$.

Curvelo, & Agnelli, 2001; Huang, Yu, & Ma, 2004; Huang et al., 2005). In spite of the higher polarity of the nanocomposites compared with the starch, the equilibrium moisture uptake was found to decrease with the amount of layered silicate added. The equilibrium moisture uptake value depends on hydrophilic character as well as on morphology (macro voids, free volume, crystal size and degree of crystallinity). The clay produces a tortuous path-way and also a diminution of the length of free way for water-uptake.

To determine the water absorption rate, the effective diffusion coefficient ($D_{eff}$) at short times was calculated from the slope in the initial linear portion of the $(w_t - w_0)/w_\infty$ vs $t^{0.5}$ plot, following Eq. (4) (Dufresne, Dupeyre, & Vignon, 2000):

$$\frac{w_t - w_0}{w_\infty} = \frac{4}{h}\left(\frac{D_{eff}}{\pi}\right)^{0.5} t^{0.5} \quad (4)$$

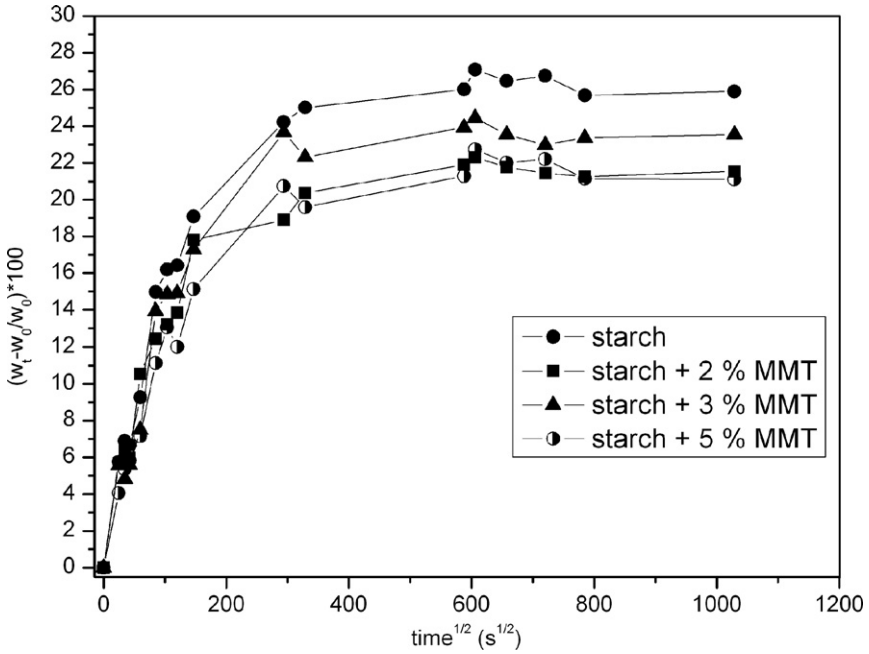


Fig. 5. Moisture absorption curves of nanocomposites films and starch.

where: $w_t$ is the wet weight of films at each time, $w_0$ is the initial weight of dry film, $w_\infty$ is the weight of the films when the maximum equilibrium water uptake was reached and $h$ is the thickness of the specimen.

In general, composites do not fulfil the requirements for using the Fick's law. Because of this, in the present work, Eq. (4) was used to calculate an effective diffusion coefficient, $D_{eff}$. This coefficient includes those factors affecting the diffusion of water such as: (a) that the composite materials are inhomogeneous; (b) there exists chemical interaction between matrix and filler with water; (c) water may diffuse through the filler-matrix interphase; (d) extractable materials can be removed during water uptake and (e) dimension of the specimens may vary during the time of the experiment.

Table 3 shows the $D_{eff}$ coefficient obtained for the starch films and their composites. It was observed that the water absorption rate is slower for the composites compared with the starch. So, the addition of MMT diminishes the rate of water uptake absorption of the starch films due to the tortuous structure formed by the clay.

The surface of the films was observed by means of transmission optical microscopy. The micrographs (Fig. 6) showed a change in the morphology of the specimen surfaces with the MMT content. On one hand, the film made of native starch contained crystals of small size all over the film. On the other hand, in the micrograph of the composites it was observed the presence of bigger crystals than those observed in the starch. However the crystallinity of the composites and the starch films was similar nearly to 0.16, calculated from the X-ray patterns. Then, it is seems that the diffusion of water depends on crystal size more than on the degree of crystallinity.

Table 3
Diffusion coefficients for the starch and nanocomposites

| Sample | Diffusion coefficient $D_{eff} \times 10^8$ (mm$^2$/s) |
|---|---|
| Starch | 2.00 |
| Starch + 2% of MMT | 1.37 |
| Starch + 3% of MMT | 1.82 |
| Starch + 5% of MMT | 1.73 |

Mechanical properties resulted from the tensile test are shown in Fig. 7 and Table 4. It was observed an important increase of five and sixfold in the modulus when 3 and 5 wt% of MMT was added to the starch, respectively. The maximum stress also showed an increment of 57% for the composite with 5 wt% of MMT compared to the starch. A similar behavior in the modulus increment was also observed by other authors (Chen & Evans, 2005; Huang et al., 2005) in plasticized starch/clay system. Huang et al. (2005) observed that the Young's modulus increased with the MMT content. However, this increment was more important when up to 5 wt% of clay was added to the starch. Then the values of Young's modulus did not follow the same trend with the addition of MMT. The slope was lower than that observed with less MMT.

This behavior was expected and was attributed to the resistance exerted by the clay itself and to the orientation and aspect ratio of the intercalated silicate layers. In addition, the stretching resistance of the oriented backbone of the polymer chain in the gallery bonded by hydrogen interaction also contributed to enhancing the modulus and the stress. The deformation decreases with the MMT content as shown in Table 4. The layered silicate acts as a mechanical reinforcement of starch reducing the flexibility of the

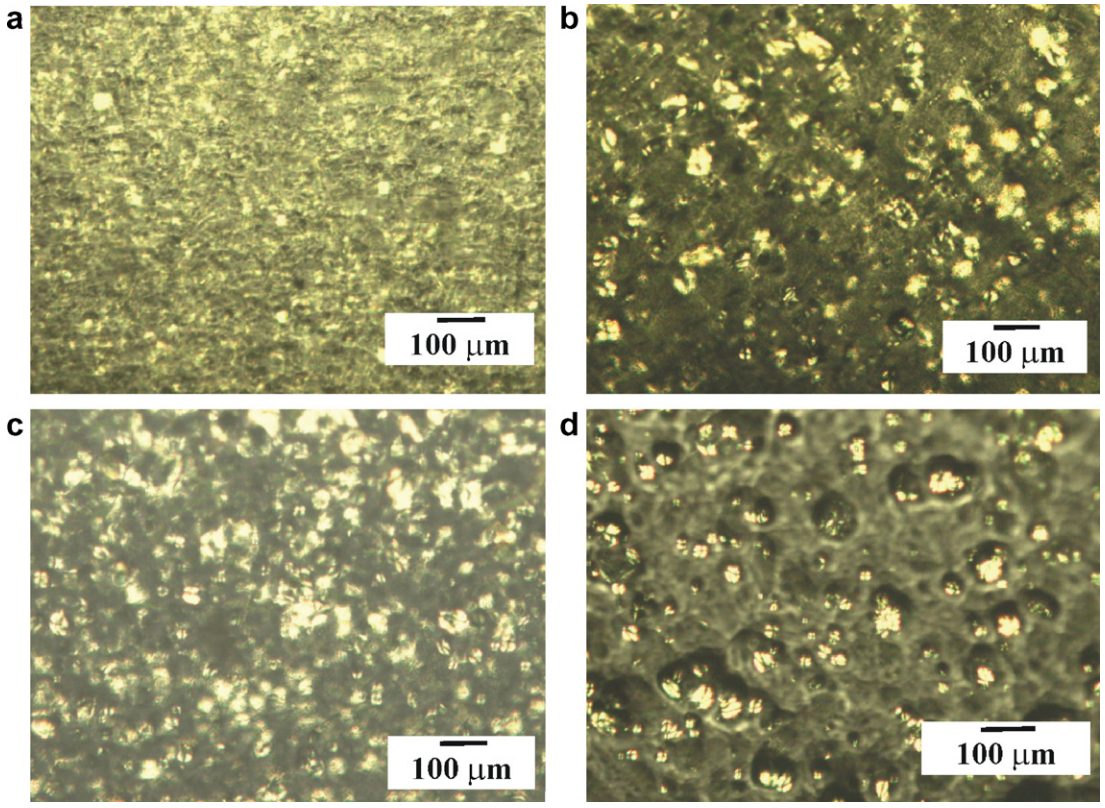


Fig. 6. Optical micrograph of the films of starch (a) and the composites with: 2 wt% (b), 3 wt% (c) and 5 wt% (d) of MMT.

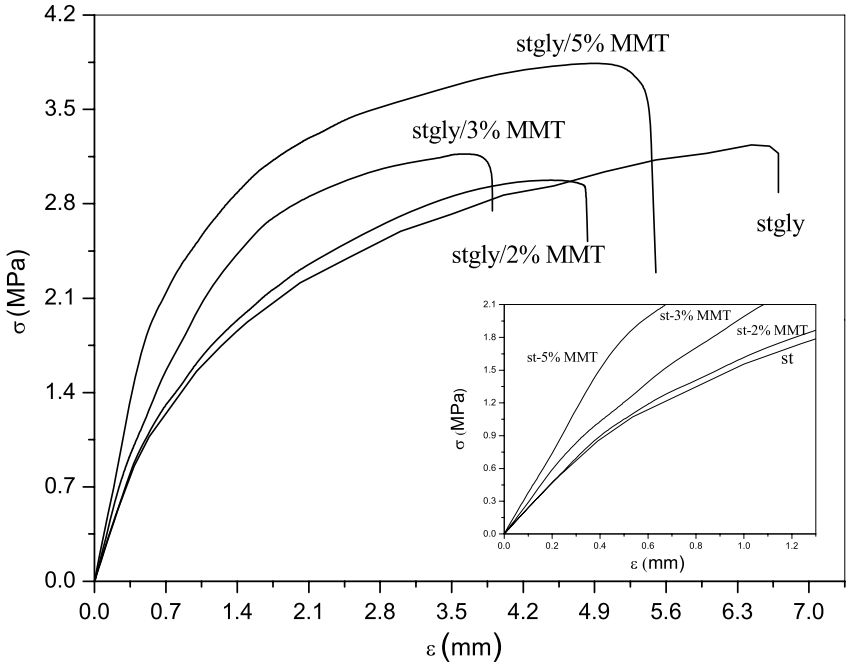


Fig. 7. Strength vs. elongation (mm) for starch/glycerol (stgly), starch/glycerol with 2 wt% MMT (stgly 2% MMT), starch/gly with 3 wt% (stgly 3% MMT) and starch/gly with 5 wt% (stgly 3% MMT).

polymer. The nanocomposites exhibited a remarkable improvement in the mechanical properties especially in the Young modulus. The main reason for this improvement in the mechanical properties is the stronger interfacial interaction between the matrix and layered silicate due to the vast surface exposed of the clay layers. SEM images of the fracture surface after tensile test were obtained for the films. The micrograph showed in Fig. 8a revealed a

Table 4
Mechanical properties of the starch and their composites

| Sample | Max stress (MPa) | Deformation at max stress (%) | Young's modulus (MPa) | Stress at break (MPa) | Deformation at break (%) |
|---|---|---|---|---|---|
| Starch | 3.3 ± 0.4 | 60.5 ± 10.7 | 29.8 ± 4.4 | 3.1 ± 0.4 | 62.6 ± 10.1 |
| Starch + 2% of MMT | 3.1 ± 0.3 | 52.8 ± 15.6 | 29.6 ± 12.1 | 2.7 ± 0.4 | 55.1 ± 17.2 |
| Starch + 3% of MMT | 3.2 ± 0.7 | 34.8 ± 14.0 | 150.5 ± 25.6 | 2.4 ± 0.7 | 37.6 ± 14.5 |
| Starch + 5% of MMT | 5.2 ± 0.8 | 40.3 ± 4.4 | 195.6 ± 38.6 | 4.1 ± 1.1 | 46.8 ± 19.2 |

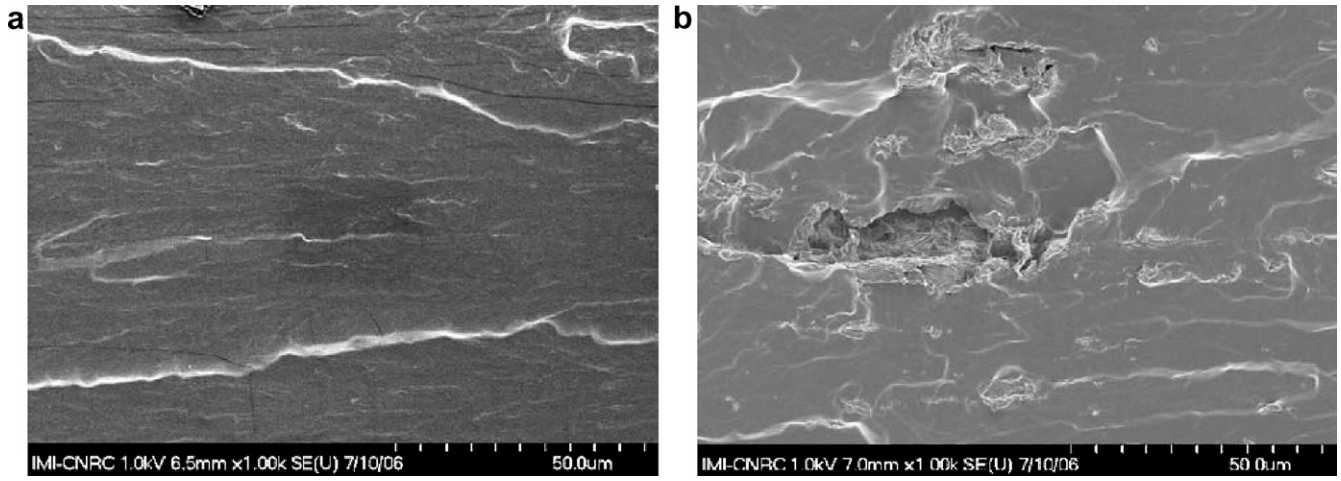


Fig. 8. SEM micrograph of starch (a) and the composites of 3 wt% of MMT (b).

smooth surface for the native starch. It was reported (Tjong, 2006) that in the intercalated nanocomposites the clay platelets are poorly dispersed and form aggregates that break upon loading, as was observed in the fracture surface of the starch composites (Fig. 8b).

## 4. Conclusions

Physical and mechanical properties of glycerol-plasticized starch/clay nanocomposites films were determined.

An increment in the interlayer distance of the clay in the nanocomposites was observed by X-ray diffraction providing evidence that the clay nanolayer formed an intercalated structure without reach a complete exfoliation.

An improvement in the thermal resistance of the starch with the addition of clay was observed by means of thermogravimetric analysis. This result indicated that the clay acts as heat barrier enhancing the overall thermal stability of the system.

The composites showed a higher hydrophilic character than the starch due to the high polarity of the MMT added. It was observed that the maximum of water uptake as well as the rate of water absorption was reduced by the addition of clay to the starch. This behavior was attributed to the structure formed between the molecules of starch and the MMT. The formation of a tortuous path-way by the presence of clay influences the rate of water-uptake. The differences in the hydrophilicity and morphology among the systems affect the equilibrium water-uptake value of the films.

The nanocomposites exhibited a remarkable improvement in the mechanical properties such as Young modulus and tensile stress. However a diminution in the deformation was observed due to the reinforcing action of MMT. The main reason for this improvement in the properties in polymer clay nanocomposites is the strong interfacial interaction between matrix and clay which has a high modulus (170 GPa) and change the morphology of the matrix of starch.

## Acknowledgments

The authors thank the financial support of CONICET and SECYT (PIP No. 6254, PICT 12-15074, PICT 14-25529 and PICT 12-14600).

## References

Bastioli, C. (1995). Starch Polymer Composites. In Degradable Polymer. Berlin: Cambridge. p. 112.

Baumberg, S., Lapierre, C., Monties, B., & Della Valle, C. (1998). Use of kraft lignin as filler for starch films. *Polymer Degradation Stability, 59*, 273.

Carvalho, A. J. F. de., Curvelo, A. A. S., & Agnelli, J. A. M. (2001). A first insight on composite of thermoplastic starch and kaolin. *Carbohydrate Polymers, 45*, 189–194.

Charles, A., Kao, H-M., & Huang, T-Ch. (2003). Physical investigations of surface membrane–water relationship of intact and gelatinized wheat–starch systems. *Carbohydrate Research, Vol. 338*(22), 2403.

Cheetham, N., & Tao, L. (1998). Variation in crystalline type with amylase content in maize starch granules: An X-ray powder diffraction study. *Carbohydrate Polymer, 36*, 277.

Chen, B., & Evans, J. (2005). Thermoplastic starch –clay nanocomposites and their characteristics. *Carbohydrate polymers, 61*, 455–463.

Cyras, Viviana P., Tolosa Zenklusen, M. Carolina., & Vázquez, Analía (2006). Relationship between structure and properties of modified potato starch biodegradables films. *Journal of Applied Polymer Science, 101*(6), 15:4313.

Dufresne, A., Dupeyre, D., & Vignon, M. (2000). Cellulose microfibrils from potato tuber cells: Processing and characterization of starch-cellulose microfibril composites. *Journal of Polymer Science, 76*, 2080.

Gutowski, W. (1991). In Lieng-Huang. Lee (Ed.), *Fundamentals of adhesion*. New York: Plenum Press (Chapter 2).

Huang, M-F., Yu, J-G., & Ma, X-F. (2004). Studies on the properties of montmorillonite-reinforced thermoplastic starch composites. *Polymer, 45*, 7017–7023.

Huang, M., Yu, J., Ma, X., & Peng, Jin. (2005). High performance biodegradable thermoplastic starch-EMMT nanoplastics. *Polymer, 46*(9), 3157.

Lin-Vien, D., Colthup, N. B., Fateley, W. G., & Grasselli, J. G. (1991). *The handbook of infrared and Raman characteristic frequencies of organic molecules*. London: Academic Press (Chapter 4).

Park, H. M., Li, X., Jin, C. Z., Park, C. Y., Cho, W. J., & Ha, C. K. (2002). Preparation and properties of biodegradable thermoplastic starch/clay hybrids. *Macromolecular Materials and Engineering, 287*, 553.

Plackett, D., & Vázquez, A. (2004). *Green composites*. Polymer composites and the environmental. In Caroline Baillie (Ed.), *Chapter 7: Natural Polymer Source* (pp. 123). Washington, DC. Cambridge. England: CRC Press.

Pukánszky, B., Müller, P., & Bagdi, K. (2006). Thermoplastic starch/layered silicate composites: structure, interaction, properties. *Composite Interfaces, Vol. 13*(1), 1–17.

Ray, S. S., & Okamoto, M. (2003). Polymer/layered silicate nanocomposites: a review from preparation to processing. *Progress in Polymer Science, 28*(11), 1539.

Shimizu, R. N., & Demarquette, N. R. (2000). Evaluation of surface energy of solid polymers using different models. *Journal of Applied Polymer Science, 76*, 1831.

Singh, R., Pandey, J., Rutot, D., Degée, Ph., & Dubois, Ph. (2003). Biodegradation of poly(ε-caprolactone)/starch blends and composites in composting and culture environments: the effect of compatibilization on the inherent biodegradability of the host polymer. *Carbohydrate Research, Vol. 338*(17), 1759.

Svensson, E., & Eliasson, A. (1995). Crystalline changes in native wheat and potato straces at intermediate water levels during gelatinization. *Carbohydrate Polymer, 26*, 171.

Tjong, S. C. (2006). Structural and mechanical properties of polymer nanocomposites. *Materials Science and Engineering, 53*, 73–197.